THE JOURNAL OF THE ACOUSTICAL SOCIETY OF KOREA Vol.29, No.1E 2010. 3. pp. 28-37

Cellular-level Biomechanics of Ultrasound

Won-Suk Ohm*
*School of Mechanical Engineering, Yonsei University
(Received February 11, 2010; accepted March 16, 2010)

Abstract

This article reviews recent developments in the emerging field of cellular-level biomedical ultrasonics with the specific focus on the mechanics of ultrasound-cell interaction. Due to the nature of the field at its relative infancy, the review poses more questions than it provides answers. Discussed are topics such as the basic structure of a biological cell, the origin of cell's elasticity, a theoretical framework for ultrasound-cell interaction, and shape deformation of cells and its measurement. Some interesting problems for future study are proposed.

Keywords: *ultrasound, cell, biomechanics, deformation, sonoporation, bubble*

I. Introduction

Interaction of ultrasound with biological cells can be viewed in the broader context of cell mechanostimulus. Mechanical stimuli such as impact, stretching and shear have been shown to facilitate proliferation, differentiation, healing or apoptosis of cells [1-3]. Among many loading modalities used for cell mechanostimulus [4], ultrasound is recently gaining popularity because of its ease of use, controllability, and noninvasiveness. Ultrasound can be administered to target cells either in vitro or in vivo, to manipulate cells [5] or to produce a host of beneficial bioeffects at the cellular level [6]. Applications of ultrasound in this vein range from needle-free transdermal drug injection [7], targeted drug delivery [8], gene therapy [9], healing of bone fracture [10], differentiation of mesenchymal stem cells [2], to ultrasound-induced apoptosis of cancer cells [3]. To have more than a glimpse of ultrasound as "healing sound," interested readers may resort to a comprehensive text edited by Wu and Nyborg [11].

Although the efficacy of ultrasound at the cellular level is undisputed, the exact mechanisms by which ultrasonic stimulus brings about cellular-level bioeffects is still shrouded in mystery. One possible scenario that has a wide acceptance among researchers is sonoporation, in which a plasma membrane deformed by ultrasound becomes more permeable to proteins, ions, drugs, and genes [6, 12-14]. The marriage between mechanics of ultrasound and biochemistry of cells is highly puzzling in its own right, and is waiting to be fully explained. What is even more urgent is the exact understanding of ultrasound-cell interaction from the purely mechanistic point of view. Without it, any attempt to understand the aforementioned coupling between mechanics and biochemistry rests on tenuous grounds. In this light this article reviews some recent developments in biomechanics with a rather narrow focus on the mechanics of cells under ultrasound exposure. The review is by no means comprehensive in the sense that it is intended to highlight only the basics of cell mechanics and the work performed by the author and a few others on

Corresponding author: Won-Suk Ohm (ohm@yonsei.ac.kr)
School of Mechanical Engineering, Yonsei University
262 Seongsanno, Seodaemun-gu, Seoul 120-749, Korea

the topic of ultrasound-induced deformation of cells. Organization of the article is as follows. First, the cell structure is reviewed from the strength-of-materials point of view in Sec. II. With the knowledge of the elasticity of cells, deformation of cells by ultrasound is discussed in Sec. III. Section IV chronicles some experimental efforts to measure cell deformation by ultrasound. Last, the list of unsolved problems in this area of research is compiled in Sec. V.

II. Elasticity of cells

Cells come in a variety of shapes, sizes and internal organizations. Although we focus here, for simplicity's sake, on cells with the simplest constitution, namely, bacteria, many of the biomechanical attributes of bacteria are representative of those of more complex cells. We also acknowledge that the description to follow is largely based on the material in Ref [15].

A bacterium, being a prokaryotic cell without internal cytoskeletal filaments, has its water-like cytoplasm contained in a cell boundary. Here, we use the term "cell boundary" rather than "plasma membrane," because a cell boundary is more than just a plasma membrane as illustrated in Fig. 1. A plasma membrane, a ubiquitous component for all cells, is a 4~5-nm thick phospholipid bilayer with embedded proteins, whose main function is to regulate the passage of molecules and ions into and out of a cell. Basically a thin fluid sheet, the plasma membrane alone cannot withstand much elevated internal (turgor) pressure nor provide structural rigidity. What reinforces the plasma membrane to give rise to elasticity in a bacterium is the cell wall, which is a two-dimensional peptidoglycan network. (For more complex cells, cell walls are made of either cytoskeletal filaments as in red blood cells or cellulose in plant cells.) The thickness of a cell wall is in the neighborhood of 20 nm for Gram-negative bacteria (e.g., *E. coli*) and can be as large as 80 nm for Gram-positive bacteria (e.g., *B. subtilis*). The cell wall is considered to be thin relative to the bacterium itself, whose typical dimension is in the order of 1~10 microns. With the reinforcement by the cell wall, the cell boundary becomes a thin shell-like elastic structure.

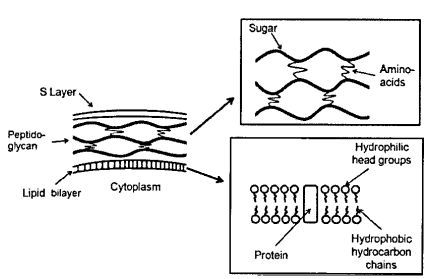

Fig. 1. Structure of the cell boundary of a Gram-negative bacterium. The insets are zoom-in views of the peptidoglycan network (upper) and the phospholipid bilayer (lower), respectively.

In the context of ultrasound-cell interaction, the cell boundary is important on two fronts. First, it is the primary source of elasticity in bacteria. The cell boundary, when deformed by ultrasound, provides most restoring force such that a cell can exhibit shape oscillation with possible resonance. On the other hand, cytoplasm, being a water-like medium, provides no restoring force, and only dissipates acoustic energy via thermoviscous effects. Second, the cell boundary is implicated in the sonoporation scenario as the major recipient of ultrasonic drive. It is the compromised permeability of the cell boundary (or the plasma membrane to be exact) that leads to increased uptake of molecules and ions.

Because the elasticity of the cell boundary is chiefly responsible for cell's overall elasticity, we now discuss how to quantify it from the strength-of-materials point of view. As mentioned earlier, the cell boundary of a bacterium can be modeled as a thin isotropic elastic shell. Thus, theory pertaining to a thin shell [16-18] can be used with little modification to capture the elastic behavior of the cell boundary. In a nutshell, two-parameter representation may suffice, where shell's elasticity is signified by

the area compression modulus K_A and the surface shear modulus μ. If we consider, for example, a spherical bacterium (or a coccus) undergoing axisymmetric deformation as in Fig. 2, the constitutive equations relating the tensions T_θ and T_φ and the strains $e_{\theta\theta}$ and $e_{\varphi\varphi}$ within the cell boundary are given by [17, 18]

$$T_\theta = K_A(e_{\theta\theta}+e_{\varphi\varphi}) + \mu(e_{\theta\theta}-e_{\varphi\varphi}) + T_0, \quad (1)$$

$$T_\varphi = K_A(e_{\theta\theta}+e_{\varphi\varphi}) - \mu(e_{\theta\theta}-e_{\varphi\varphi}) + T_0, \quad (2)$$

where T_0 is the turgor pressure of the bacterium. Note that the term $(e_{\theta\theta} + e_{\varphi\varphi})$ in Eqs. (1) and (2) denotes the relative area change of an infinitesimal surface element, whereas the term $(e_{\theta\theta} - e_{\varphi\varphi})$ signifies the area-preserving pure shear deformation. Because the number and size of pores in the plasma membrane seem to increase with the area of the membrane [12, 13], the relative area change $(e_{\theta\theta} + e_{\varphi\varphi})$ along with the area compression modulus K_A may be used to quantify the magnitude of sonoporation.

One final note on the elasticity of cells: the physical origin of the elasticity in cells is not only the work required to deform the cell wall but also the tendency to resist entropy loss due to deformation [15]. Straightening out a cell wall reduces the number of configurations that a peptidoglycan network can assume, and therefore entails an entropy loss. And it is the resistance to the deformation-induced entropy loss that gives rise to elasticity in the polymeric network of peptidoglycan. In contrast to soft materials like cells, the elasticity of hard materials such as steel arises almost entirely from the work required to produce deformation. This can be demonstrated from the first law of thermodynamics written as

$$\Delta\varepsilon = T\Delta s + \sigma_{ij}\Delta e_{ij}, \quad (3)$$

where ε is the internal energy stored in the shell, T the absolute temperature, s the specific entropy, σ_{ij} and e_{ij} the stresses and strains within the shell. As one would expect from the 1st law of thermodynamics, the products $T\Delta s$ and $\sigma_{ij}\Delta e_{ij}$ in Eq. (3) represent the heat (hence entropy change) and the work given to the shell, respectively. Now note that the energy expenditure $\Delta\varepsilon$ on shell deformation is the sum of the work $\sigma_{ij}\Delta e_{ij}$ and the entropy change $T\Delta s$. The entropic contribution to elasticity is significant in soft materials such as polymers, whereas it is of minimal importance for hard materials. The constitutive relations for cells [Eqs. (1) and (2)] contain both contributions to elasticity, which are couched in the two elasticity parameters K_A and μ.

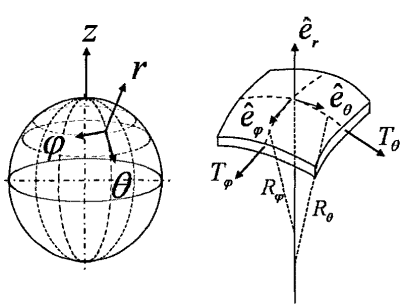

Fig. 2. Coordinate system on a spherical shell and the tensions T_φ and T_θ acting on a differential surface element of the spherical shell.

III. Deformation of cells by ultrasound

Prediction and measurement of ultrasound propagation in tissues are greatly facilitated by the fact that a tissue, with the exception of bones, often behaves as a water-like homogeneous medium. A tissue, which is a dense aggregate of similar cells, exhibits acoustic properties close to those of water. Therefore, both analysis and measurement can be performed using water as the propagation medium, followed by an ad hoc augmentation of tissue-specific attenuation. An example of this is the acou-

stic intensity measurement in diagnostic ultrasound, where intensity values measured in water are processed with the 0.3-dB/cm-MHz derating factor as per specified by the AIUM/NEMA standard [19]. However, when it comes to studying the interaction of ultrasound with suspended cells as in a cell culture, a different approach is required because suspended cells act as a loose collection of tiny scatterers, with their elasticity originating from the shell-like cell boundary. In other words, cells in suspension are quite similar to droplets in an immiscible host fluid, except the fact that in the case of droplets the restoring force against deformation arises from the surface tension at the droplet boundary.

In this section, we start with a theoretical framework called the thin-shell model for describing the ultrasound-induced deformation of a cell suspended in a host liquid [17, 18]. Consider a spherical cell composed of the cytoplasm (the inner liquid) and the cell boundary (the thin shell) immersed in a host liquid (the outer liquid) as shown in Fig. 3. Either an incident plane wave or a secondary sound emission from a nearby bubble drives the cell into motion. The cell responds with its own sound radiation in the form

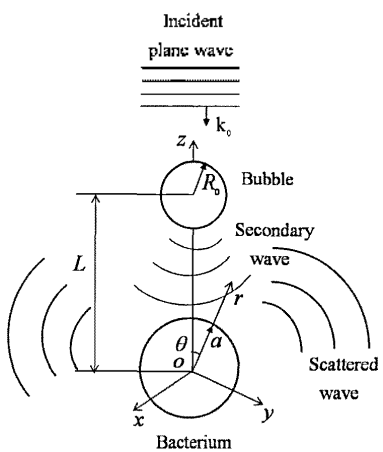

Fig. 3. Schematic view of a cell being driven by an incident plane wave and (or) the secondary spherical wave from a nearby bubble. Dimensions including the wavelengths of the waves are not to scale.

of scattered waves, while undergoing deformation. This interaction can be stated mathematically as follows. The acoustic field in the outer liquid is given by the sum of the incident wave and its scattered components:

$$\Phi^o = \Phi^{inc} + \Phi^s, \tag{4}$$

where the symbols Φ^o, Φ^{inc}, and Φ^s denote scalar velocity potentials for the outer liquid, the incident wave, and the scattered wave, respectively. Here, velocity potentials Φ^{inc} and Φ^s can be written in the spherical coordinates as [20]

$$\Phi^{inc}(r,\theta) = \sum_{n=0}^{\infty} E_n j_n(k_o r) P_n(\cos\theta) e^{-i\omega t}, \tag{5}$$

$$\Phi^s(r,\theta) = \sum_{n=0}^{\infty} A_n h_n(k_o r) P_n(\cos\theta) e^{-i\omega t}, \tag{6}$$

where n is the mode number, j_n the spherical Bessel function, h_n the spherical Hankel function, P_n the Legendre polynomial, ω the forcing frequency, t time, k_o the wavenumber for the outer fluid. Coefficients E_n and A_n are the amplitudes of the nth mode partaking in Φ^{inc} and Φ^s, respectively. Once the remaining three velocity potentials (scalar potential Φ^i for the inner liquid and two vector potentials A^o and A^i) are expanded in a similar way, there are four undetermined coefficients A_n, B_n, C_n, and D_n for each mode. Application of boundary conditions at the cell boundary ($r = a$) yields a system of four algebraic equations in the unknown coefficients for each n:

$$G_n x_n = y_n, \tag{7}$$

where G_n is a 4×4 system matrix, $x_n = [A_n\ B_n\ C_n\ D_n]^T$ the solution vector, and y_n is the forcing vector depending on coefficients E_n. The system matrix G_n is a function of material properties of the inner and outer liquids, the dimension and elastic moduli of the shell, and the forcing frequency. Equation (7) is the

dynamical equation in matrix form, describing the motion (or deformation) of a suspended cell by ultrasound. Further details of the theoretical development are found in Refs. [17, 18]. Given Eq. (7), two important parameters that characterize the dynamics of a suspended cell, namely, the natural frequency and the quality factor of vibration are sought. To obtain these two parameters we consider the free vibration problem [Eq. (7) with $y_n = 0$]. The free vibration problem has a nontrivial solution only if the system matrix G_n becomes singular. Thus, the natural frequency and the quality factor are given by the root(s) of the dispersion relation:

$$\det(G_n) = F(\omega_n) = 0. \tag{8}$$

At this juncture, it must be pointed out that the dominant mode of cell vibration is that of a lateral quadrupole ($n = 2$), which has the cloverleaf radiation pattern as depicted in Fig. 4 (a). To see why, imagine a water-filled balloon immersed in water, which serves as a mimic of a cell suspended in a liquid. Because water inside the balloon is a very hard medium to compress (or expand), it would be very difficult to drive the water-filled balloon in the monopole mode of vibration ($n = 0$, omni-directional pulsation) as shown in Fig. 4 (b). Likewise, excitation of the dipole mode ($n = 1$, back-and-forth translational motion) is equally difficult, because the whole balloon must be displaced against the inertia of the surrounding water. As for the quadrupole mode, however, a gentle squeeze and release is sufficient enough to set the balloon in motion such that it shrinks around the equator while bulges at the poles and vice versa [see Fig. 4 (a)]. We hereafter focus solely on the quadrupole mode of vibration.

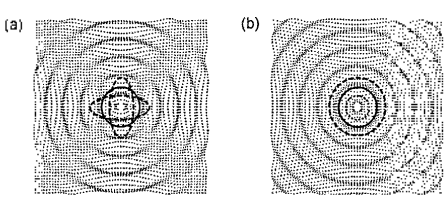

Fig. 4. Different modes of cell deformation: (a) the quadrupole ($n = 2$) vs. (b) the monopole ($n = 0$) mode. Solid lines represent the cell shape prior to deformation, while dashed lines show the modes of deformation. Part of the figure (radiation patterns in the background) is the courtesy of Dr. Dan Russell, Kettering University (http://paws.kettering.edu/~drussell/demos.html).

Natural frequencies f_2 and associated quality factors Q_2 for the quadrupole mode ($n = 2$) are obtained numerically from the dispersion relation [Eq. (8)] [17, 18, 21], and the results for a few types of cells are listed in Table 1 [21]. The following observations are made from Table 1:

- Natural frequencies of bacteria range from ~100 kHz to ~20 MHz. Thus the frequency of mechanical resonance of a cell is far greater than that of thermal fluctuation, which is in the order of ~1 kHz [22].
- A cell can have more than one natural frequency for the quadrupole mode of vibration [21]. This is a significant finding that is not widely appreciated by researchers in this field.
- Cells with very small elasticity such as the protoplast (a cell with its cell wall removed) of *N. tabacum* may have no natural frequency at all [21]. The dynamical response of these cells is completely relaxational.
- A cell may exhibit both high- and low-quality resonances as exemplified by the case of *B. emersonii* ($Q_2 = 16.0$ at 2.24 MHz and 0.9 at 24.2 MHz).

To study the deformation of a cell by ultrasound one ought to solve the full dynamical equation [Eq.

Table 1. Natural frequencies and quality factors for a few types of cells [21].

CELL TYPE	f_2 (MHz)	Q_2
B. yeast	0.16	1.6
	0.584	0.6
B. emersonii	2.24	16.0
	24.2	0.9
N. tabacum (protoplast)	none	none

(7) with $y_n \neq 0$]. In doing so, a proper choice of acoustic drive y_n for E_n in Eq. (5)] is crucial, because the magnitude of the cell's response could be dramatically different from one acoustic input to the other. To showcase this point we compare the effectiveness of two acoustic inputs, i.e., an incident mono-frequency plane wave and the secondary spherical wave emitted by a pulsating microbubble adjacent to the cell (see Fig. 3). Note that the pulsation of the bubble results from the incident plane wave. These two acoustic inputs can be written as Eq. (5) with the coefficients E_n given by

$$E_n = \frac{1}{\omega}\sqrt{\frac{2Ic_o}{\rho_o}}\, i^{n} \quad (2n+1) \tag{9}$$

for the incident plane wave, and

$$E_n \quad \omega \frac{\Delta R}{R_o} k_o R_o^3 (2n+1) h_n(k_o L) \tag{10}$$

for the secondary spherical wave from the bubble [18]. Here, I denotes the acoustic intensity of the incident plane wave, c_0 and ρ_0 the sound speed and density of the outer liquid, R_0 the equilibrium radius of the bubble, ΔR the maximum excursion of bubble radius, and L the average distance between the bubble and the cell. Figure 5 compares the strengths of the two acoustic drives for the excitation of the quadrupole mode (that is, the coefficients E_2) when the intensity of the incident wave is 10 mW/cm^2 [21]. It is apparent from Fig. 5 that an oscillating bubble is a far more effective acoustic driver of the cell, where the coefficient E_2 of the bubble (dotted line) is at least four orders-of-magnitude greater than that of the plane wave (solid line) over the frequency range of interest.

The ineffectiveness of a mono-frequency plane wave in driving cells can be explained via comparison of the wavelength of the plane wave with the cell dimension. For example, the wavelength of a plane wave at the first natural frequency of *B. emersonii* in water is approximately 0.7 mm, which is about two orders-of-magnitude larger than the radius of the cell (a = 10 microns). Because the scattering cross-section of the cell is so small compared to the wavelength, the acoustic energy of the plane wave is not well coupled to the resonant deformation of the cell. On the contrary, the spherical wave radiated by a nearby bubble is more attuned to the shape and dimension of the cell such that it can lead to a substantial level of deformation, causing membrane rupture and cell lysis under certain circumstances.

Figure 6 shows the maximum relative area change of *B. emersonii*, plotted against forcing frequency for the plane and the secondary spherical waves [21]. Again, the relative area change $\Delta S/S$ is defined as

$$\frac{\Delta S}{S} \sim e_{\theta\theta} + e_{\phi\phi}, \tag{11}$$

where $e_{\theta\theta}$ and $e_{\phi\phi}$ are the strains in the θ and ϕ axes, respectively. The relative area change is an appropriate measure of cell deformation, because the quadrupole mode, being an isochoric (volume-preserving) deformation, manifests itself as the change in area of the cell boundary. In Fig. 6, the deformation by the bubble, amounting to a few percent, is about a thousand times larger than that by the plane wave alone. Membrane rupture may

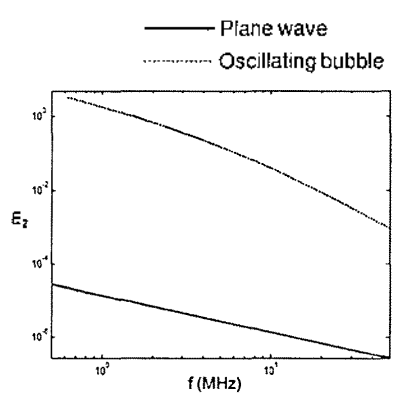

Fig. 5. Coefficients E_2 as a function of frequency for two different acoustic drives: plane wave (solid) vs. secondary spherical wave from an oscillating bubble (dotted) [21].

occur at relative area change as low as 5% [17]. What is interesting in Fig. 6 (a) is the existence of the second low-quality resonance near 25 MHz following the first high-quality resonance at about 2 MHz. This corroborates the prediction of two natural frequencies (2.24 MHz and 24.2 MHz) with dramatically different quality factors (16.0 and 0.9) as shown in Table 1.

IV. Measurement

So far relatively few experimental studies have addressed the measurement of ultrasound-induced cell deformation per se. Instead, only telltale signs of ultrasound action such as membrane wounds, the uptake of macromolecules, and the resulting bioeffects were measured and reported. Besides, a sheer majority of these studies involved microbubbles as

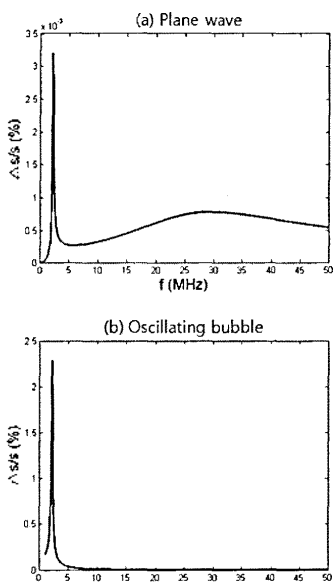

Fig. 6. Calculated frequency response of *B. emersonii* in terms of the maximum relative area change of the cell boundary by (a) a plane wave and (b) the secondary spherical wave from a neighboring bubble [21]. The acoustic intensity is 10 mW/cm^2.

an intermediary for exciting cells, whether intended or not. This underscores a multitude of difficulties associated with exciting and capturing the cell motion in real time.

One study that dealt with the aftermath of ultrasound action is that by Schlicher et al [13]. These investigators applied ultrasound to DU 145 prostate-cancer cells to observe the resulting membrane disruption and the uptake of molecules. Cell cultures were sonicated with a tone burst at 24 kHz, 7 atm, and 10% duty cycle. Although no artificial microbubbles such as ultrasound contrast agent (UCA) were added to cell cultures, the mechanical index (MI) for the ultrasound exposure was approximately 4.5, which was high enough to allow cavitation inception and even violent bubble motion within samples. Therefore, the primary mechanism of ultrasound action was most likely the inertial cavitation and the microjetting of asymmetrically collapsing bubbles [7]. Following ultrasound exposure, samples were photographed using SEM, TEM, and confocal microscopy. Figure 2 in Ref. [13] shows some of the SEM and TEM images of the sonicated cell (the second and third columns) against those of the control (the first column). From the SEM images [Figs. (a2) and (a3) in the first row], one can clearly see the extent of damage on the plasma membrane due to ultrasound exposure: a patch of membrane was torn away, exposing cytoskeleton inside the cell (indicated by arrows). The violence of action presumably by a nearby collapsing bubble was such that the size of the membrane breach almost measured a few microns [see Fig. (a3)]. The last row of TEM images [Figs. (c2) and (c3)] also show the membrane disruption along with tiny vesicles (indicated by arrows), believed to be involved in active membrane resealing.

Perhaps most visually stunning is the work by van Wamel et al. [23], where the deformation of endothelial cells by ultrasonically-driven microbubbles was recorded with a high-speed camera with the rate of 10 million frames per second. In their in vitro experiment, the cell culture treated with microbubbles

was placed inside an Opticell™ container, and the ultrasound bubble cell interaction was photographed with a high-speed camera mounted in line with a microscope. The ultrasound exposure protocol consisted of a 1-MHz tone burst with the peak negative pressure of 0.9 MPa, generated by a single-element transducer. The microbubbles used were lipid-coated ultrasound contrast agent (Sonovue™), whose bubble spectrum ranged from 1 micron to 12 microns. As microbubbles pulsate next to endothelial cells, changes in cross-sectional cell dimension of up to 15% were observed. The recorded image sequence of cell's deformation produced by ultrasound-bubble-cell interaction is shown in Fig. 2 in Ref. [23].

By now a keen reader might ask "Do bubbles always have to be an integral part of ultrasound-cell interaction?" Or "Is there any ultrasound exposure protocol that can excite cells without the aid of microbubbles?" A possible answer may lie in the use of modulated radiation pressure as proposed in Ref. [17]. In it, acoustic radiation pressure in a standing wave field is amplitude-modulated in such a way that the wavelength of the carrier corresponds to the dimension of the cell, while the frequency of modulation is that of the quadrupole resonance of the cell. This technique was successfully used in an earlier study for exciting the quadrupole oscillation of immiscible drops of size in the order of mm [24].

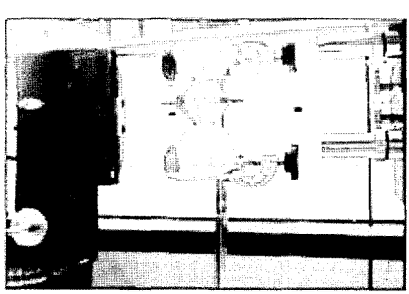

Fig. 7. Experimental setup for exciting and measuring ultrasound-induced deformation of cells [21]. For detection of cell deformation, we are trying to carefully "listen to" acoustic emissions from vibrating cells with a hydrophone.

but has not been extended to the case of micron-sized cells.

The author's group at Yonsei University is approaching the problem from an entirely different angle. A snapshot of the experiment in progress is shown in Fig. 7. Our two-pronged approach includes (a) a bubble-independent ultrasound exposure protocol for excitation of cells and (b) an experimental recipe to synchronize the acoustic responses from cells for enhanced acoustic detection. Sound radiation by a quadrupole source is very weak compared to that of a monopole [20]. Thus synchronization of the acoustic emissions from cells may be necessary to raise the amplitude of the acoustic signature above the noise floor. Synchronization of acoustic sources has been studied by a number of researchers in attempts to create UASER (Ultrasound Amplification by Stimulated Emission of Radiation), an acoustic analog to laser [25]. In view of suspended vibrating cells as a three-dimensional distribution of quadrupole sound sources, we are hoping in some foreseeable future to come up with a recipe for UASER based on biological cells.

V. Uncharted waters

Cellular-level ultrasound medicine is going to be the next frontier of biomedical ultrasound. There is a long and tortuous road ahead till the cellular-level ultrasound medicine is accepted as widely as diagnostic ultrasonic imaging today. Efficacy and safety must be further established on firm theoretical and clinical foundations. In this regard, the author proposes some important problems for future work on the biomechanics side.

- Excitation and measurement of cell deformation: The key constraint here is ultrasound-only excitation. Excitation aided by microbubbles is shown to be highly effective in driving cells. However, bubbles are sometimes a mixed blessing

in that (a) bubbles are hard to manipulate and (b) bubbles can cause significant damages to cells even at moderate levels of acoustic intensity. Therefore an ultrasonic exposure protocol that is independent from bubbles will be a welcome development in terms of simplicity and safety.

- Modeling of more complex cells: Spherical bacteria account for only a small fraction of cells, where nature is populated with about 200 different types of cells. It would be an interesting exercise to extend the thin-shell model [17, 18] to accommodate cells with slightly more complex shapes such as red blood cells (RBCs). Red blood cells have been studied extensively, hence exists a wealth of information regarding their geometry and deformability. Also, RBCs have particular significance from the medical standpoint.
- Development of cellular-level safety/efficacy index: One of the major vehicles that accelerated the commercial success of diagnostic ultrasound is the stipulation of real-time display of ultrasound safety indices, namely, MI and TI [26]. In the same vein, a safety/efficacy index at the cellular level may help the future success of cellular-level ultrasound medicine. A preliminary study on this end has been performed by the author's group at Yonsei University and the colleagues at Korea Research Institute of Standards and Science [21]. The so-called cell stimulation index (CSI) proposed in Ref. [21] is defined as

$$CSI = \frac{\Delta S/S}{(\Delta S/S)_{\max}}, \tag{12}$$

where $\Delta S/S$ is the aforementioned relative area change that can be computed through the thin-shell model. The parameter $(\Delta S/S)_{\max}$ is the relative area change at the onset of membrane rupture, which differs from cell to cell but is often in the neighborhood of 10%. According to the above definition, CSI of unity serves as the demarcation point that distinguishes stimulation and disruption regimes: CSI less than unity implies stimulation by ultrasound, whereas CSI greater than unity means disruption of the cell.

Acknowledgement

This work was supported by the Korea Research Council of Fundamental Science and Technology (KRCF) through Basic Research Project by the Korea Research Institute of Standards and Science (KRISS).

The author thanks Youngsoo Choi, Hunki Lee, and Jae-Wan Lee for drawing figures.

References

1. T.-J. Kim, S.-J. Kim, and H.-I. Jung, "Physical stimulation of mammalian cells using micro-bead impact within a microfluidic environment to enhance growth rate," *Microfluid. Nanofluid.*, vol. 6, no. 1, pp. 131-139, 2009.
2. K. Ebisawa, K.-I. Hata, K. Okada, K. Kimata, M. Ueda, S. Torii, and H. Watanabe, "Ultrasound enhances transforming growth factor β-mediated chondrocyte differentiation of human mesenchymal stem cells," *Tissue Eng.*, vol. 10, no. 5/6, pp. 921-929, 2004.
3. Y. Furusawa, Q.-L. Zhao, M. A. Hassan, Y. Tabuchi, I. Takasaki, S. Wada, and T. Kondo, "Ultrasound-induced apoptosis in the presence of Sonazoid and associated alterations in gene expression levels: A possible therapeutic application," *Cancer Lett.*, vol. 288, no. 1, pp. 107-115, 2010.
4. T. D. Brown, "Techniques for mechanical stimulation of cells in vitro: a review," *J. Biomech.*, vol. 33, no. 1, pp. 3-14, 2000.
5. T. Laurell, F. Petersson, and A. Nilsson, "Chip integrated strategies for acoustic separation and manipulation of cells and particles," *Chem. Soc. Rev.*, vol. 36, no. 3, pp. 492-506, 2007.
6. S. Mitragotri, "Healing sound: the use of ultrasound in drug delivery and other therapeutic applications," *Nature Rev. Drug Discov.*, vol. 4, no. 3, pp. 255-260, 2005.
7. M. Ogura, S. Paliwal, and S. Mitragotri, "Low-frequency sonophoresis: current status and future prospects," *Adv. Drug Deliv. Rev.*, vol. 60, no. 10, pp. 1218-1223, 2008.
8. N. Y. Rapoport, D. A. Christensen, H. D. Fain, L. Barrows, and Z. Gao, "Ultrasound-triggered drug targeting of tumors in vitro and in vivo," *Ultrasonics*, vol. 42, no. 1-9, pp. 943-950, 2004.
9. H. Azuma, N. Tomita, Y. Kaneda, H. Koike, T. Ogihara, Y. Katsuoka, and R. Morishita, "Transfection of NFκB-decoy oligodeoxynucleotides using efficient ultrasound-mediated gene transfer into donor kidneys prolonged survival of rat renal allografts," *Gene Ther.*, vol. 10, no. 5, pp. 415-425, 2003.
10. M. Hadjiargyrou, K. McLeod, J. P. Ryaby, and C. Rubin, "Enhancement of fracture healing by low intensity ultrasound," *Clin. Orthop. Rel. Res.*, vol. 355, suppl., pp. S216-S229, 1998.

11. J. Wu and W. Nyborg, eds., *Emerging Therapeutic Ultrasound*, World Scientific, New Jersey, 2006.
12. K. Tachibana, T. Uchida, K. Ogawa, N. Yamashita, and K. Tamura, "Induction of cell-membrane porosity by ultrasound," *Lancet*, vol. 353, no. 9162, p. 1409, 1999.
13. R. K. Schlicher, H. Radhakrishna, T. P. Tolentino, R. P. Apkarian, V. Zarnitsyn, and M. R. Prausnitz, "Mechanism of intracellular delivery by acoustic cavitation," *Ultrasound Med. Biol.*, vol. 32, no. 6, pp. 915-924, 2006.
14. J. Wu and W. L. Nyborg, "Ultrasound, cavitation bubbles and their interaction with cells," *Adv. Drug Deliv. Rev.*, vol. 60, no. 10, pp. 1103-1116, 2008.
15. D. Boal, *Mechanics of the Cell*, Cambridge University Press, Cambridge, 2002.
16. L. D. Landau and E. M. Lifshitz, *Theory of Elasticity, 3rd ed.*, Butterworth-Heinemann, Oxford, 1986.
17. P. V. Zinin, J. S. Allen II, and V. M. Levin, "Mechanical resonances of bacteria cells," *Phys. Rev. E*, vol. 72, no. 6, paper no. 061907, 2005.
18. P. V. Zinin and J. S. Allen III, "Deformation of biological cells in the acoustic field of an oscillating bubble," *Phys. Rev. E*, vol. 79, no. 2, paper no. 021910, 2009.
19. AIUM/NEMA, *Standard for real-time display of thermal and mechanical acoustic indices on diagnostic ultrasound equipment*, AIUM, Laurel, MD, 1998.
20. D. T. Blackstock, *Fundamentals of Physical Acoustics*, Wiley, New York, 2000.
21. W.-S. Ohm, Y. Choi and Y.-T. Kim, "Development of cellular-level efficacy/safety index for biomedical ultrasound," Korea Research Institute of Standards and Science, Tech. Rep., 2009.
22. A. E. Pelling, S. Sehati, E. B. Gralla, J. S. Valentine, J. K. Gimzewski, "Local nanomechanical motion of the cell wall of Saccharomyces cerevisiae," *Science*, vol. 305, no. 5687, pp. 1147-1150, 2004.
23. A. van Wamel, A. Bouakaz, M. Versluis, and N. de Jong, "Micromanipulation of endothelial cells: ultrasound-microbubble-cell interaction," *Ultrasound Med. Biol.*, vol. 30, no. 9, pp. 1255-1258, 2004.
24. P. L. Marston and R. E. Apfel, "Quadrupole resonance of drops driven by modulated acoustic radiation pressure-experimental properties," *J. Acoust. Soc. Am.*, vol. 67, no. 1, pp. 27-37, 1980.
25. I. V. Volkov, S. T. Zavtrak, and I. S. Kuten, "Theory of sound amplification by stimulated emission of radiation with consideration for coagulation," *Phys. Rev. E*, vol. 56, no. 1, pp. 1097-1101, 1997.
26. J. G. Abbott, "Rationale and derivation of MI and TI-a review," *Ultrasound Med. Biol.*, vol. 25, no. 3, pp. 431-441, 1999.

[Profile]

• Won-Suk Ohm

received his B.S. degree in mechanical engineering from Korea Advanced Institute of Science and Technology in 1994, and M.S. and Ph.D. degrees in mechanical engineering from the University of Texas at Austin in 1997 and 2001, respectively. He was a visiting scientist at the Institute for National Measurement Standards, National Research Council of Canada from 2002 to 2005, and a senior engineer at Medison Co., Ltd. in Korea from 2006 to 2008. In 2008, he joined the faculty in the School of Mechanical Engineering at Yonsei University in Korea. His research interest ranges from biomedical ultrasonics, underwater acoustics, to acoustical metrology.